Cellulose (2021) 28:3265–3277
https://doi.org/10.1007/s10570-021-03716-x

ORIGINAL RESEARCH

Enhancing antibacterial and flame-retardant performance of cotton fabric with an iminodiacetic acid-containing *N*-halamine

Denghui Xu · Shijie Wang · Jiewen Hu · Yun Liu · Zhiming Jiang · Ping Zhu

Received: 6 September 2020 / Accepted: 22 January 2021 / Published online: 16 February 2021

Abstract This research focused on preparing antibacterial and flame-retardant multifunctional cotton fabric to decrease the threat of harmful microorganism and fire, which might have huge potential application in household textiles. A water-soluble *N*-halamine precursor based on s-triazine (TIAPC) was synthesized by introducing iminodiacetic acid (IDA), which can chelate with metal ions to obtain flame retardancy. After coating with TIAPC, the cotton fabric was chlorinated in dilute bleach solution and chelated in metal salt solution to achieve antibacterial and flame-retardant properties. The surface morphology and chemical state of TIAPC-coated cotton fabric were characterized by FT-IR, XPS, SEM and EDX. The chlorinated TIAPC-coated cotton fabric displayed high-efficacy and rapid bactericidal effect against *S. aureus* and *E. coli* O157: H7 with 100% bacterial reduction in 1 min. Meanwhile, the chelated TIAPC-modified cotton fabric presented good thermal stability and char-forming capability. The hydrophobic property of modified cotton fabric was greatly improved after chlorination. Besides, this multifunctional coating had little effect on the cytotoxicity, tensile strength, air permeability, whiteness and drape of cotton fabric.

Supplementary Information The online version contains supplementary material available at https://doi.org/10.1007/s10570-021-03716-x.

D. Xu · S. Wang · J. Hu · Y. Liu · Z. Jiang (✉) · P. Zhu (✉)
Institute of Functional Textiles and Advanced Materials, College of Textile and Clothing, State Key Laboratory of Bio-Fibers and Eco-Textiles, Qingdao University, Qingdao 266071, China
e-mail: jzm070315@163.com

P. Zhu
e-mail: pzhu99@163.com

Graphic abstract

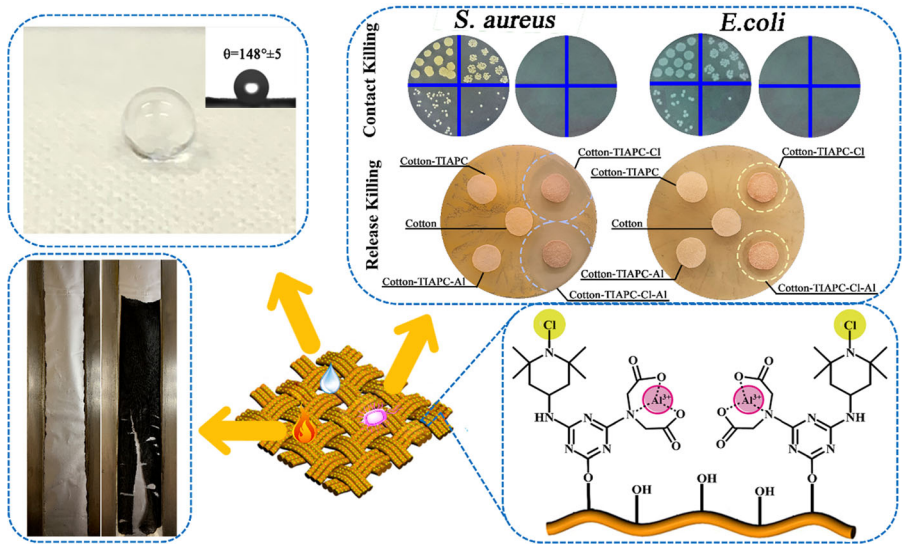

Keywords Cotton fabric · *N*-halamine · Metal ion · Antibacterial · Flame retardant

Introduction

To prevent and control emerging diseases, numerous researchers are devote to the development of efficient antibacterial technologies. As a new kind of antibacterial agent, *N*-halamines possess the characteristics of ideal antibacterial agent, such as rapid disinfection, long-term stability, broad-spectrum activity, safety and regenerability (Yin et al. 2020). In the last several decades, *N*-halamines have attracted significant research interest and been extensively applied to prepare efficient antimicrobial textiles, which can protect people from harmful microorganisms (Wen et al. 2020; Zhang et al. 2019). Except for avoiding cross-infection of diseases, introducing *N*-halamines can prevent microorganisms from deteriorating physical–mechanical properties and producing unpleasant odors of textiles (Bai et al. 2016).

In the early 1990s, Sun et al. prepared antibacterial cotton fabrics with *N*-halamine precursor, 1,3-dihydroxymethyl-5,5-dimethylhydantoin (DMDMH), and durable and excellent biocidal performance was obtained after exposing to dilute household bleach except for formaldehyde emission (Sun et al. 2001). Then, formaldehyde-free *N*-halamines attracted significant research interest. Many kinds of *N*-halamine precursors with different reactive groups, such as double bond (Ren et al. 2009; Sun and Sun 2002), siloxane bond (Ren et al. 2008; Worley et al. 2005) and epoxy group (Cerkez et al. 2012; Kocer et al. 2011), were developed and applied to fabricate durable and desirable antibacterial textiles. However, considering eco-friendly preparation process and practical application, reactive *N*-halamine precursors with good water solubility should be more attractive and worthy because harmful organic solvents can be avoided in the finishing process.

In recent years, some quaternarized *N*-halamine precursors, such as 3-chloro-2-hydroxypropyl)-(5,5-dimethylhydantoinyl-1-ylmethyl)-dimethylammonium chloride (CDDAC) (Kang et al. 2013) and (5,5-dimethylhydantoinyl-3-ylethyl)-dimethylamine (DEADH) (Zhang et al. 2013), were designed to enhance water solubility and antimicrobial efficacy. Also, antibacterial cotton fabrics can be prepared with cationic/anionic water-soluble *N*-halamine polymers through layer-by-layer technology (Li et al. 2019). In our previous studies, some *N*-halamine precursors (BTMPT, ATDT) based on s-triazine were prepared by introducing water-soluble groups such as sulfanilic acid and taurine (Jiang et al. 2014; Xu et al. 2020),

which rendered cotton fabrics with highly effective biocidal properties. On this basis, introducing other water-soluble groups, which can improve the inherent flammability of cotton, should be an efficient way to further broaden its application in the safe protection field.

Iminodiacetic acid (IDA) is a flexible diaryl ligand with good water-solubility, which can form stable chelates with many metal ions (Razak et al. 2018), and has enormous potential for use in electroplating process (Sosa et al. 2016), water treatment (Razak et al. 2018; Zhou et al. 2018) and dyeing (Acikel et al. 2017; Omer et al. 2020). It has been found that metal ions or metal salt can improve the thermal stability and combustion performance of flammable materials, which opens up a new field for preparing flame retardant materials (Zhang et al. 2016). Richards et al. found that metal ions introduced into cotton fibers through ion exchange can effectively increase the char-forming properties of cotton fiber (Richards and Zheng 1991). The influence of Na^{+}, Ca^{2+} and Zn^{2+} on flame retardancy in cellulose fibers was investigated by Xia's group. They verified that these metal ions can form barrier layers on the cellulose fiber surface, which excludes oxygen, restricts the release of gas and produces more carbon residues (Shi et al. 2017; Zhang et al. 2016).

In this study, a water-soluble *N*-halamine precursor based on s-triazine (TIAPC) was synthesized by introducing iminodiacetic acid and coated on cotton fabrics for improving antibacterial properties and flame retardancy. The introduction of iminodiacetic acid not only increased the water-solubility, but also improved the thermal stability and char-forming properties of cotton fabrics by chelating with metal ions. The surface morphology and chemical state of TIAPC-coated cotton fabrics were marked by FT-IR, XPS, SEM and EDX. Meanwhile, the antibacterial properties, combustion behavior, and thermal stability of TIAPC-coated cotton fabrics were investigated. Besides, the cytotoxicity of TIAPC-coated cotton fabrics was evaluated by cell viability testing. The effect of TIAPC coating on the intrinsic properties of cotton fabrics, such as water contact angle, tensile strength, air permeability, whiteness, and drape, was also evaluated.

Experiment

Reagents and materials

Desized, scoured and bleached cotton fabrics (122 $g \cdot m^{-2}$) were provided from Qingdao Fenghuang Dyeing & Printing Co., Ltd., China. Cyanuric chloride (CC) and 0.1 N $Na_2S_2O_3$ were provided by J&K Scientific Co., Ltd, China. IDA was purchased from TCI Chemical Industry Development Co., Ltd, China. 4-amio *N*-2,2,6,6-tetramentylniperidine (TEMP) was obtained from Shanghai Macklin Biochemical Co., Ltd, China. KI, NaCl, $Al_2(SO4)_3$, Na_2CO_3 and hydrochloric acid were purchased from Sinopharm Chemical Reagent Co., Ltd, China. All reagents were used directly without further purification.

Synthesis of TIAPC

The intermediate, 1,3,5-triazine-2-iminodiacetic acid-4,6-dichloride (TIAC), was synthesized according to previously published literature (Huang et al. 2013). The synthesis route of 1,3,5-triazine-2-iminodiacetic acid-4-(2,2,6,6-tetramethyl-4-piperidine)-6-chloride (TIAPC) was presented Fig. 1.

0.22 mol cyanuric chloride was mixed with 150 mL deionized water in a 500 mL four-necked flask equipped with a mechanical stirrer, a thermometer and a constant pressure drop funnel, which was cooled to 0–5 °C. The mixture of 0.2 mol IDA and 0.3 mol Na_2CO_3 in 150 mL deionized water was added dropwise to the flask within 2 h at 0–5 °C. After complete addition, the mixture was maintained at 0–5 °C for another 3 h and filtered to remove the residual cyanuric chloride. Then, the pH of filtrate was adjusted to 3 with concentrated HCl solution and an amount of NaCl was added. After stirring at 0–5 °C for 30 min, the mixture was filtered and the intermediate product (TIAC) was obtained with a yield of 80.4%. The structure of intermediate TIAC was confirmed by NMR and FT-IR. ^{1}H-NMR (400 MHz, D_2O) δ (ppm): 4.41. ^{13}C-NMR (100 MHz, D_2O) δ (ppm): 50.5, 165.5, 169.7, 172.5. FT-IR (cm^{-1}): 3419, 2989, 1710, 1566, 1489, 1397, 1228, 1175, 985, 848, 736.

Then, 0.2 mol TIAC and 150 mL of deionized water were fed into a 500 mL four-necked glass flask equipped with a mechanical stirrer, a thermometer and a constant pressure dropping funnel, which was heated up to 40–45 °C. 0.2 mol TEMP in 50 mL deionized

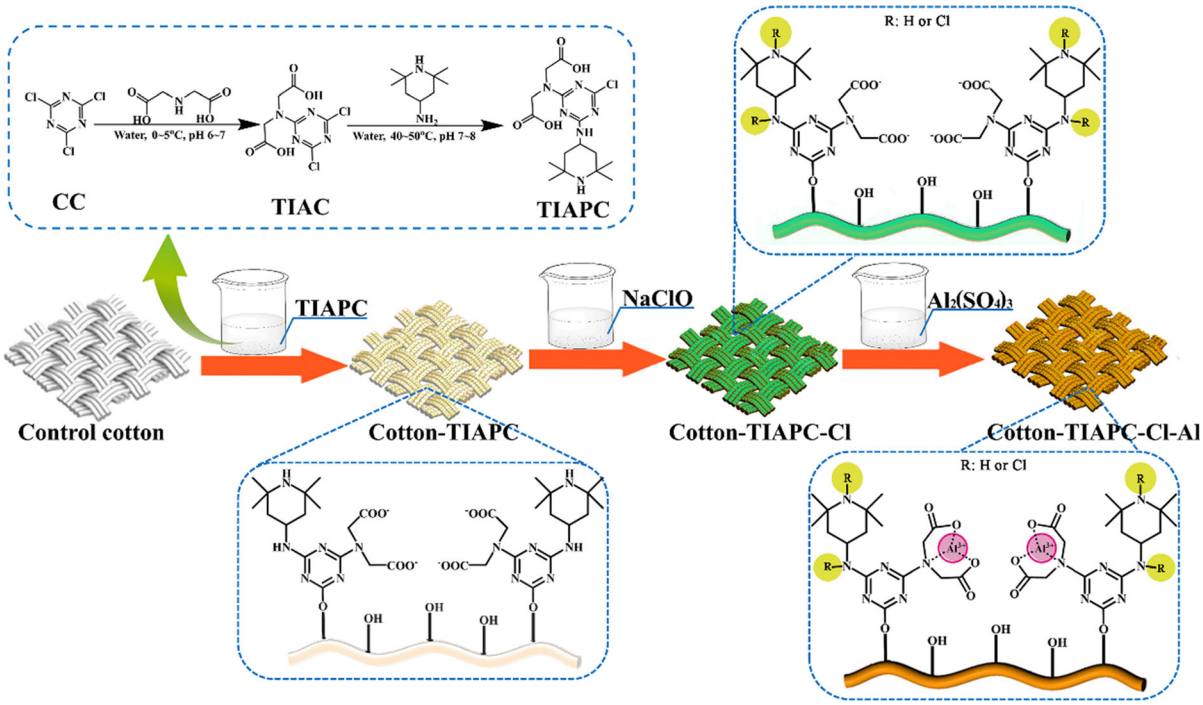

Fig. 1 Synthesis route of TIAPC and preparation of multifunctional cotton fabric

water was then added dropwise within 2 h, and the mixture was maintained at 40–45 °C for another 3 h. After the pH of the mixture adjusted to 5, the mixture was stirred at room temperature for 20 min. Then, the white product (TIAPC) was obtained with a yield of 65.7% after filtering and drying at 45 °C for 1 h. The structure of TIAPC was confirmed by NMR and FT-IR. ^{1}H-NMR (400 MHz, D_2O) δ (ppm): 1.23–1.55 (m, 14H), 1.87–1.98(m, 4H), 3.98–4.12 (d, 4H), 4.13–4.28 (m, 1H), 8.17–8.23(d, 1H). ^{13}C-NMR (100 MHz, D_2O) δ (ppm): 26.5, 32.5, 40.1, 56.2, 59.4, 166.8, 167.2, 170.7, 174.8. FT-IR (cm^{-1}): 3318, 2981, 2941, 1566, 1497, 1401, 1254, 1033, 804, 534.

Sample preparation

The cotton fabrics were soaked in deionized water for 10 min to remove some impurities, rinsed with tap water several times, dried and weighed.

The cotton sample was immersed in a 15% NaOH solution for 2 h and padded with one nip to achieve a wet pick-up of 150%. The sample was then immersed in a pH = 7.5, 20% TIAPC solution for 30 min with two dips and two nips to achieve a wet pick-up of 100%. Then the sample was dried at 100 °C for 5 min and then cured at 150 °C for 5 min. After washing with tap water thoroughly and drying at 45 °C for 1 h, the coated cotton sample designated as Cotton-TIAPC was obtained with 7.2% of weight gain.

To obtain antibacterial sample, the Cotton-TIAPC was soaked in 10 wt % aqueous sodium hypochlorite solution (the pH was adjusted to 7 using dilute HCl solution) under room temperature for 1 h. Then, the chlorinated Cotton-TIAPC samples, denoted as Cotton-TIAPC-Cl, were obtained after washing thoroughly with deionized water and dried at 45 °C for 1 h. The active chlorine content of Cotton-TIAPC-Cl was determined by the iodometric/thiosulfate titration method and calculated according to the following equation:

$$Cl^{+}\% = (N \times V \times 35.45 \times 100)/(2 \times W)$$

where $Cl^{+}\%$ is the weight percent of oxidative chlorine on the Cotton-TIAPC-Cl, N and V are the normality (equiv/L) and volume (L) of the titrant $Na_2S_2O_3$ solution, respectively, and W is the weight (g) of the Cotton-TIAPC-Cl.

To render cotton samples with flame retardancy, the Cotton-TIAPC-Cl was immersed in a 5 wt% aluminum sulfate solution at room temperature for 2 h.

Then the sample was washed thoroughly with distilled water and dried at 45 °C for 1 h. The Al^{3+} chelated Cotton-TIAPC-Cl sample was denoted as Cotton-TIAPC-Cl-Al. Besides, the Cotton-TIAPC sample chelated with Al^{3+} was designated as Cotton-TIAPC-Al.

Measurement and characterization

The Fourier Transform Infrared Spectrometer (FT-IR) of TIAPC, control cotton, and TIAPC-coated cotton fabrics before and after chelation/chlorination were characterized by Nicolet iS 50 infrared spectrometer (Thermo Fisher Scientific, USA).

^{1}H-NMR and ^{13}C-NMR spectra of TIAPC were recorded on a Bruker AVANCE III HD 400 MHz spectrometer (Bruker, Germany) and DMSO was used as a solvent.

The surface morphology and elemental compositions of all cotton samples were examined using a TESCAN VEGA3 scanning electron microscope (TESCAN, Czechoslovakia) coupling with an E1856-C2B energy-dispersive X-ray analysis (EDAX, USA) with an accelerating voltage of 11.0 kV.

X-ray photoelectron spectra (XPS) of control cotton, TIAPC-coated cotton fabrics before and after chelation/chlorination were recorded with a KRATOS AXIS-ULTRA DLD high-performance imaging X-ray photoelectron spectrometer (SHIMADZU, Japan), using an Al K X-ray source (1486.8 eV).

In vitro antibacterial tests of all cotton samples were challenged with *S. aureus* and *E. coli* O157: H7 by colony-counting methods according to a modified AATCC Test Method 100–2012 (Chen et al. 2020b). Briefly, an aliquot of 25 μL of the bacterial suspensions (10^7 CFU/mL) was added to the middle of two pieces of 2.54 cm × 2.54 cm square cotton samples and held by a sterile weight to ensure sufficient contact with the bacteria. After a certain contact time (1, 5, 10 min), the cotton samples were quenched by 5 mL of sterile 0.05 N sodium thiosulfate solution (2.5 mL of PBS and 2.5 mL of 0.1 M of $Na_2S_2O_3$ solution) to neutralize any oxidative chlorine. After vortex for several minutes, the solution was serially diluted with PBS solution. Then, the dilution was plated on trypticase soy agar plates and survival colonies were counted after incubation at 37 °C for 24 h.

The inhibition zone of uncoated and TIAPC-coated cotton fabric was evaluated against *S. aureus* and *E. coli* according to AATCC-147 (Demir et al. 2017). Briefly, *S. aureus* and *E. coli* were suspended in 100 μL phosphate buffer (pH = 7.4) to produce a suspension of a known population (10^7 CFU/mL). Then, an aliquot of 100 μL of the bacterial suspension was evenly plated on soy agar plates. All cotton samples were cut into disc with a diameter of 1.5 cm and placed onto the trypticase soy agar plates. After incubation at 37 °C for 24 h, the inhibition zone around the disc was observed.

The cytotoxic effect of the TIAPC-coated fabrics was assessed with NIH3T3 mouse fibroblasts, which were seeded on 24 well plates with a density of 2×10^4 cells per well and cultured in a humidified environment at 37 °C and 5% CO_2 for 24 h. After washing twice with phosphate buffer saline, 500 μL MTT solution (5 mg/mL) was added to each well and continue incubating for 4 h. The absorbance was measured at 570 nm using a full-wavelength EPOCH2T reader. To demonstrate repeatability, each experiment was repeated three times and the cell viability was expressed as the percentage to the control cells.

The burning performance of the uncoated and TIAPC-coated cotton samples was investigated by vertical flammability test (VFT), limiting oxygen index (LOI) and Thermogravimetric (TG). The VFT was measured according to GB/T 5455–2014 with a LFY-601A vertical combustion device (Shandong Textile Research Institute, China). All cotton samples with 300 × 89 mm^2 in size were arranged vertically, and the bottom of cotton sample was exposed to flame for 12 s. The LFY-606B digital limiting oxygen index apparatus (Shandong Institute of Textile Science, China) was used to test the LOI values according to GB/T 5454-1997, and the test size of all cotton samples was 150 × 98 mm^2. TG was carried out on a thermogravimeter (TG209F3, Netzsch, Germany) from room temperature to 800 °C at a heating rate of 10 °C /min under nitrogen atmosphere.

The water contacting angle (WCA) was measured using a WCA measurement device (Theta, Biolin, Sweden). The air permeability of control cotton and Cotton-TIAPC-Cl-Al was measured according to GB/T 5453–1997 method using a YG461E-III fully automatu permeability instrument (Ningbo Textile Instrument Factory) with a pressure applied of 100 Pa. The whiteness of control cotton and Cotton-TIAPC-Cl-Al was measured by X-rite 8400 colorimeter (X-

rite, America). The tensile strength and breaking elongation of control cotton and Cotton-TIAPC-Cl-Al were measured on a YG065H series strength tester (Laizhou Electron Instrument Co. Ltd., China) according to GB/T 3923.1–1997 method. Besides, the storage stability of Cotton-TIAPC-Cl-Al was measured by detecting oxidative chlorine loading and whiteness. The tensile strength after 25 storage days was also determined and the sample was marked as Cotton-TIAPC-Cl-Al-S. The washing stability of Cotton-TIAPC-Cl-Al was assessed by detecting oxidative chlorine loading and LOI values.

Results and discussions

Structural characterization of TIAPC

The molecular structure of TIAPC was characterized via FT-IR, ^{1}H-NMR and ^{13}C-NMR spectra (presented in Fig. 2). Figure 2a showed the FT-IR spectrum of TIAPC, the characteristic absorption peaks for TIAPC were attributed as follows: 3318 cm^{-1} ($V_{–NH–}$), 534 cm^{-1} and 1033 cm^{-1} ($V_{tr\text{-}Cl}$, tr meant triazine ring here) (Xu et al. 2020), 1497 cm^{-1} and 804 cm^{-1} (V_{tr}) (Wang et al. 2018), 1566 cm^{-1} ($V_{–N=C–}$), 1254 ($V_{–C–N–}$) (Lai et al. 2012), 1713 cm^{-1} ($V_{–C=O–}$) (Kagarise 1955), which indicates that the TIAPC was successfully obtained.

NMR technology was used to further verify the molecular structure of TIAPC, Fig. 2b, c showed the ^{13}C-NMR and ^{1}H-NMR of TIAPC, respectively. The ^{13}C-NMR spectrum of TIAPC shows the following proton signals δ (ppm): 26.5 (a), 32.5 (b), 40.1 (c), 56.2 (d), 59.4 (e), 166.8 (g), 167.2 (f), 170.7 (h), 174.8 (i). In addition, the ^{1}H-NMR spectrum of TIAPC shows the following proton signals δ (ppm): 1.23–1.55 (14H, 1 and 2), 1.87–1.98 (4H, 2), 3.98–4.12 (4H, 3), 4.13–4.28 (1H, 4), 8.17–8.23 (1H, 5). Therefore, all of the above NMR assignment indicates that the TIAPC was successfully synthesized.

Characterization of TIAPC-coated cotton fabrics

FT-IR, SEM–EDX and XPS were used to access the difference of surface appearance and chemical composition between uncoated and TIAPC-coated cotton fabric. Figure 3f presents the FT-IR spectra of control cotton, Cotton-TIAPC, Cotton-TIAPC-Cl, Cotton-TIAPC-Al, and Cotton-TIAPC-Cl-Al. Compared with control cotton, there are two new characteristic peaks that were observed at 810 cm^{-1} and 1580 cm^{-1} after coating with TIAPC, which belong to skeleton vibration of triazine ring and the vibration of COO^{-} group (Viola et al. 2019; Xu et al. 2020). Besides, the peaks at 1540 cm^{-1} and 1506 cm^{-1} were attributed to the deformation vibration of two types of secondary amine groups (-NH-) in piperidine amine. After chlorination, one type of N–H was changed to N-Cl, as evidenced by the disappearance of the peak at 1540 cm^{-1}. The slight increase in the intensity of characteristic peaks (the other amine groups) from 1506 to 1525/1528 cm^{-1} may be caused by the formation of quaternary amine and hydrogen bond (Hanshaw et al. 2008; Hisaki et al. 2012; Mazik and Cavga 2006).

To observe the coating growth and element distribution of TIAPC-coated cotton fabrics, the scanning electron microscopy (SEM) and energy-dispersive X-ray spectroscopy (EDX) were employed to analyze

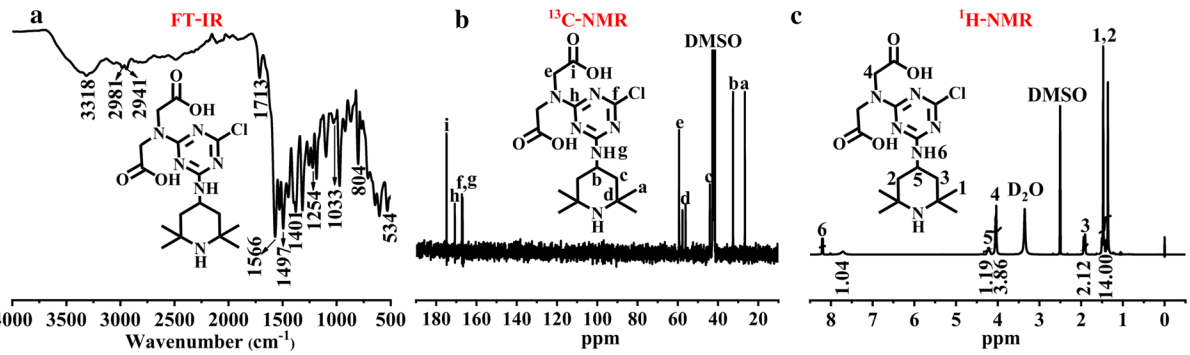

Fig. 2 FT-IR spectra (**a**), ^{13}C-NMR spectra (**b**) and ^{1}H-NMR spectra (**c**) of TIAPC

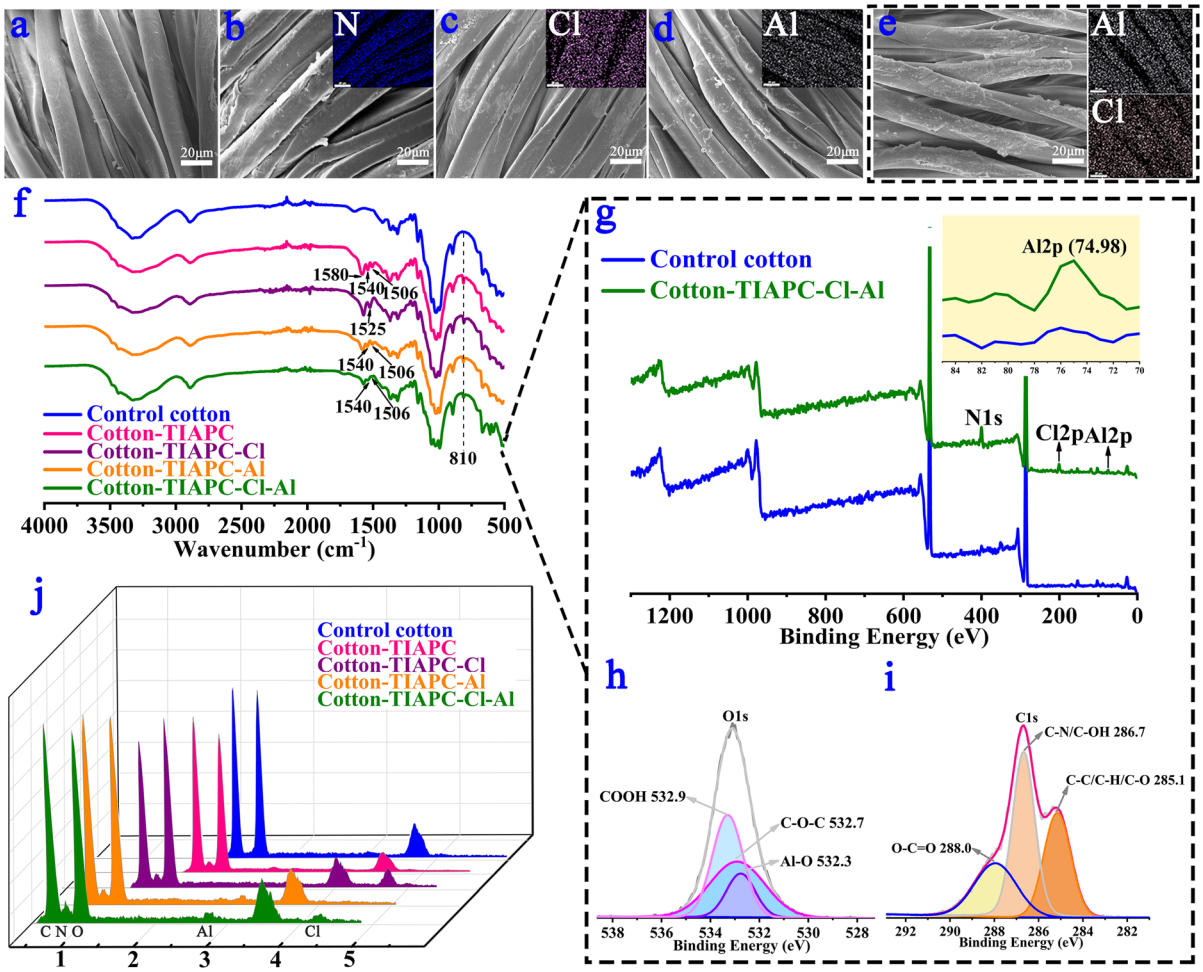

Fig. 3 SEM photographs EDX mapping of Control cotton (**a**), Cotton-TIAPC (**b**), Cotton-TIAPC-Cl (**c**), Cotton-TIAPC-Al (**d**) and Cotton-TIAPC-Cl-Al (**e**); FT-IR spectra (**f**) and 3D EDX spectra (**j**) of different cotton samples; high-resolution spectra O1*s* (**h**) and C1*s* (**i**) of Cotton-TIAPC-Cl-Al

the surface morphology and chemicals on the surface of uncoated and TIAPC-coated cotton fiber. As shown in Fig. 3a, control cotton showed a smooth surface, the TIAPC-coated cotton fabrics (Fig. 3b, c, d and e) have similar structure and shape, but the rougher morphological characteristics might be due to a thin TIAPC film formed on the cotton fiber (Zhu et al. 2020). From the results of EDX in Fig. 3j, a large number of N elements were detected on the surface of TIAPC-coated cotton fabric, which further proved that TIAPC was coated on the surface of fiber. After chlorination, a little amount of evenly distributed Cl elements was found on Cotton-TIAPC-Cl and Cotton-TIAPC-Cl-Al, which proved that parts of N–H structure on TIAPC was successfully converted into N-Cl structure. Cotton-TIAPC-Al and Cotton-TIAPC-Cl-Al had a few amounts of Al elements, which were evenly distributed on the fibers. The above differences between uncoated and TIAPC-coated cotton fabrics indicted that TIAPC was successfully coated on the cotton surface of cotton fabric.

To further confirm TIAPC, Cl and Al existed on cotton fabric, XPS measurements were performed and the results were shown in Fig. 3g–i. Compared with control cotton, three new characteristic peaks at 399.5 eV (N1*s*), 200.4 eV (Cl2*p*) and 75.0 eV (Al2*p*) of Cotton-TIAPC-Cl-Al were detected, indicating the presence of N, Al and Cl on the surface of coated sample. The O1*s* spectrum (Fig. 3h) of Cotton-TIAPC-Cl-Al could be deconvoluted into three

individual component groups (COOH, C–O–C, and Al–O) at 532.9, 532.7 and 532.3 eV, respectively (Chen et al. 2020a; Zhang et al. 2018). Figure 3i displayed high-resolution C1s spectra with three main components deconvoluted at 288.0, 286.7, and 285.1 eV, which were assigned to the O–C=O, C–N/C–OH and C–C/C–H/C–O, respectively (El-Nahhal et al. 2003). The above result proved that chlorination and chelation happened in Cotton-TIAPC-Cl-Al.

Antimicrobial assay

A combined biocidal mechanism of *N*-halamines, including contact and release killing, has been proposed (Ahmed et al. 2009). To investigate the antibacterial mechanism of TIAPC-coated cotton fabric, the antimicrobial efficacy and inhibitory zone were evaluated in this study.

The antibacterial efficacy was measured against *S. aureus* and *E. coli* O157: H7, and the results are presented in Fig. 4a, b and S1. Control cotton, Cotton-TIAPC and Cotton-TIAPC-Al showed a slight reduction of bacteria after 10 min of contact time, which might be due to the adhesive of bacteria on the cotton samples. The chlorinated sample, Cotton-TIAPC-Cl and Cotton-TIAPC-Cl-Al, displayed high-efficiency and rapid bactericidal effect, all of the bacteria could be killed within one minute, which proved that *N*-halamine owns excellent contact sterilization mechanism (Tian et al. 2017).

To further verify the release-killing mechanism of *N*-halamines, the inhibition zone test was employed to evaluate the antibiotics of TIAPC-coated cotton fabric, and the results are shown in Fig. 4c. Compared with cotton fabrics without chlorination, Cotton-TIAPC-Cl and Cotton-TIAPC-Cl-Al samples show significant inhibition zones around the sample disc. The results indicated that *N*-halamine-containing cotton fabric kills bacteria by at least some of oxidizing chlorine diffused from materials.

To evaluate the potential of new materials in biomaterial applications, the cytotoxicity was performed with NIH3T3 mouse fibroblasts by MTT assay. As shown in Fig. 4d, the cell viability of Control cotton, Cotton-TIAPC and Cotton-TIAPC-Al was excellent, indicating that the introduction of TIAPC and Al^{3+} did not affect the cell cytotoxicity. However, the chlorinated samples exhibited a

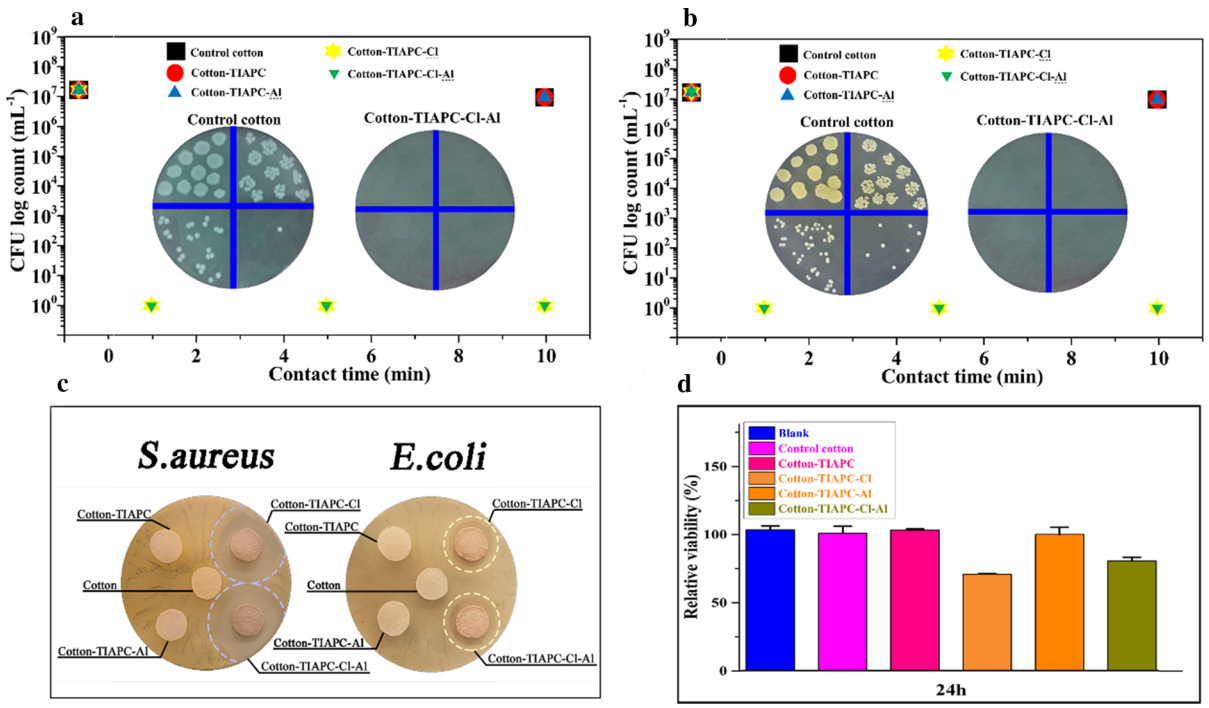

Fig. 4 Antimicrobial efficacy (*S. aureus* (**a**) and *E. coli* (**b**)), inhibition zone (**c**) and cytotoxic effect (**d**) of Control cotton, Cotton-TIAPC, Cotton-TIAPC-Cl, Cotton-TIAPC-Al and Cotton-TIAPC-Cl-Al

significant decrease, which might be related to the surface hydrophilicity different from the tissue culture plate (Ma et al. 2013).

Combustion behavior and thermal stability

To evaluate the combustion behavior of TIAPC-coated cotton fabrics, the VFT and LOI were investigated. Figure 5 shows the digital photos of control cotton, TIAPC-coated cotton fabrics before and after chelation/chlorination after VFT. In this test, the effect of different metal ions (Cu^{2+}, Ca^{2+}, Al^{3+}, Zn^{2+}, Mg^{2+}, Fe^{3+}) on the flame retardancy of cotton fabric was investigated and the result was presented in Fig. S2. Only Al^{3+} chelated samples remained large amounts of residue after combustion, although it cannot pass the VFT with afterflame phenomenon. For the samples of Cotton-TIAPC-Al, Cotton-TIAPC-Cl-Al, the char-forming properties and LOI were improved. This might be due to the Al^{3+} on the surface of cotton fabric was pyrolyzed to metal oxide acting as a barrier to oxygen and heat on the surface of fibers (Pan et al. 2017). Moreover, SEM and EDX analyses were carried out to investigate the appearance

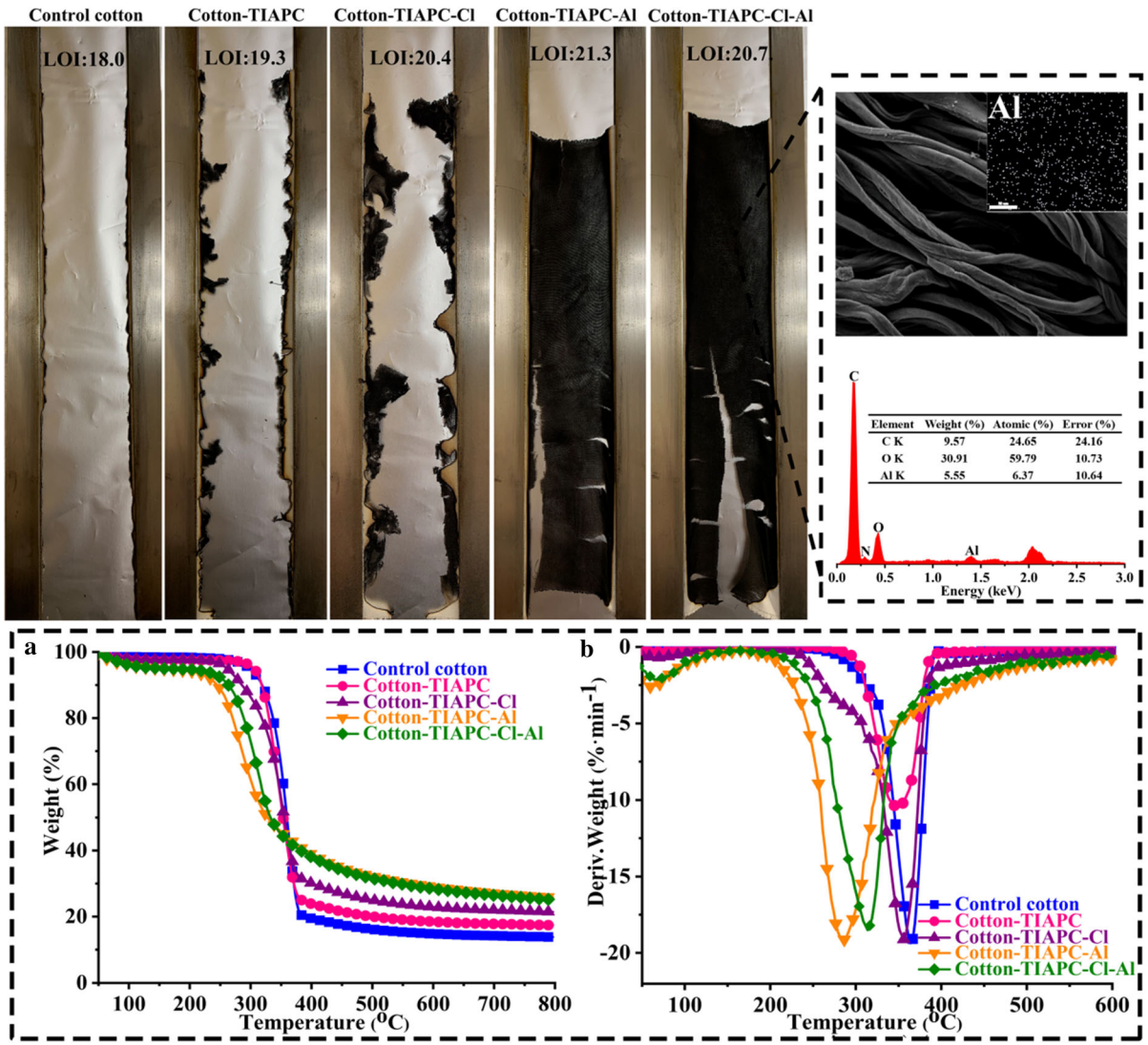

Fig. 5 Digital photographs of uncoated and TIAPC-coated cotton fabrics after VFT; TG (**a**) and DTG (**b**) curves of control cotton and TIAPC-coated cotton fabrics in the N_2

and elemental composition of char residue. After combustion, the intact wave structure was retained and the elements of Al were uniformly dispersed on the char residue of Cotton-TIAPC-Cl-Al, which further indicates that chelated metal ions can greatly improve the char-forming of cotton fabric.

The thermal stability of TIAPC-coated cotton samples was measured, and the TG curves were shown in Fig. 5a, b. Compared with control cotton, the maximum weight loss temperature (T_{max}) of Cotton-TIAPC and Cotton-TIAPC-Cl had a little change and the residue increased due to the introduction of nitrogen and chlorine elements. After chelating with Al^{3+}, lower T_{max} and more residue were observed, which is mainly due to the catalytic dehydration and carbonization of metal ions (Pan et al. 2017).

Water contact angle, tensile strength, air permeability, whiteness and drape

The water contact angle (WCA) of TIAPC-coated fabrics was checked and the result was presented in Fig. 6. The sample of Cotton-TIAPC showed similar hydrophilic surface with control cotton, but the chlorinated sample (Cotton-TIAPC-Cl) owned excellent hydrophobic performance with WCA of 152°. The chelation had little effect on the hydrophobicity of cotton sample and WCA of Cotton-TAPC-Cl-Al decreased to 148°, which might be due to a small reduction of active chlorine during the chelation process.

Tensile strength and breaking elongation of Control cotton and Cotton-TIAPC-Al-Cl were measured and the result was presented in Fig. 7. 90% of tensile strength was maintained in warp and weft directions for Cotton-TIAPC-Cl-Al. The slight reduction might be due to the loss of intermolecular/intramolecular hydrogen bonds and the substitution of hydroxyl groups on the cotton fabrics under alkaline conditions (Mu et al. 2018). However, the breaking elongation of Cotton-TIAPC-Cl-Al had a significant increase, which might be due to the stable cross-linking of TIAPC with cotton fabrics, giving the cotton fabric good ductility (Jahangiri et al. 2018). Besides, the tensile strength of Cotton-TIAPC-Cl-Al after storage (marked as Cotton-TIAPC-Cl-Al-S) was also investigated and the results showed that short-term storage had no impact on the tensile strength and breaking elongation of Cotton-TIAPC-Cl-Al.

Air permeability, whiteness, draping coefficient and draping were also investigated and the results were given in Table 1. Due to the chemical deposition onto the surface resulting in less air space between cotton fibers, the air permeability had a small reduction and 80% was remained. However, the whiteness and drape of Cotton-TIAPC-Cl-Al has little effect, which might be explained by the possibly due to high curing temperature (Xu et al. 2020).

Conclusions

A water-soluble *N*-halamine precursor (TIAPC) was successfully synthesized and characterized by FT-IR and NMR, and bond onto cotton fabrics. The cotton fabric coated with TIAPC was chlorinated with dilute bleach and chelated in metal salt solution to achieve antibacterial and flame retardant performance. The chlorinated TIAPC-coated cotton fabrics show highly-efficient and rapid bactericidal efficacy against *S. aureus* and *E. coli* O157: H7, and all of the bacteria could be killed within 1 min of contact time. The antibacterial samples also presented release-killing mechanism that was proved by the inhibition zone test. Meanwhile, the chelated TIAPC-coated cotton fabric presented good thermal stability and char-forming

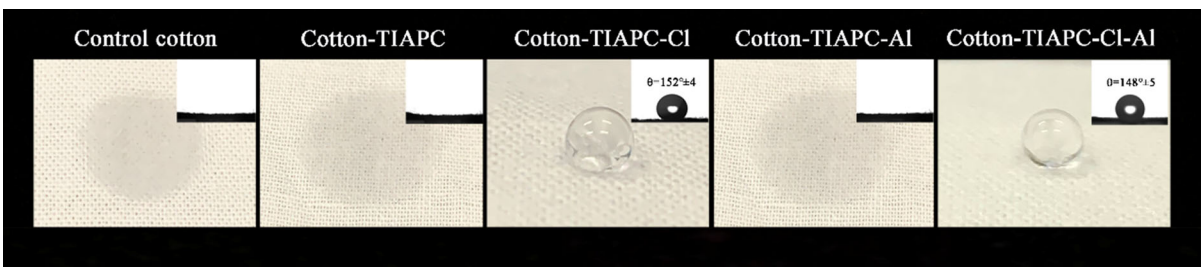

Fig. 6 Water contact angle of control cotton and TIAPC-coated cotton fabrics

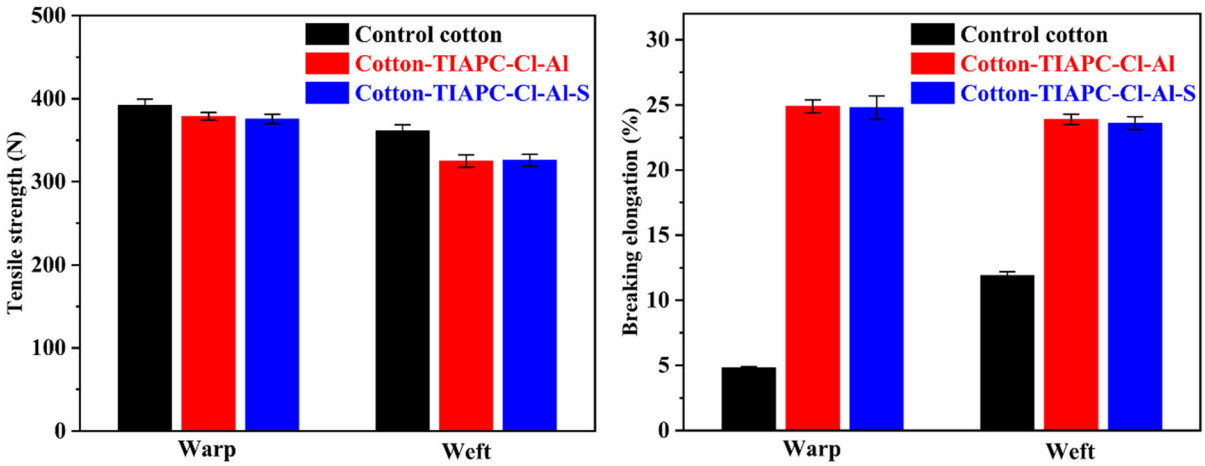

Fig. 7 Tensile strength and breaking elongation of Control cotton, Cotton-TIAPC-Cl-Al and Cotton-TIAPC-Cl-Al-S

Table 1 Air permeability, whiteness, draping coefficient and draping of uncoated cotton and Cotton-TIAPC-Cl-Al

Samples	Air permeability (mm/s)	Whiteness (%)	Draping coefficient (%)	Draping (%)
Cotton-control	416.5 ± 7.2	97.1	61.56	38.44
Cotton-TIAPC-Cl-Al	329.3 ± 8.1	72.6	71.58	28.42

capability, which was caused by chelating with metal ions. The hydrophobicity of TIAPC-modified cotton fabric was greatly improved after chlorination, which is due to the transformation of N–H to N-Cl. Besides, the TIAPC coating had little effect on the cytotoxicity, tensile strength, air permeability, whiteness and drape. However, the flame retardant performance of TIAPC-coated cotton fabric is unsatisfactory, which will be further improved in our following researches.

Acknowledgments The authors would like to thank the National Natural Science Foundation of China (51703101, 51991354).

Compliance with ethical standards

Conflict of interest The authors declare that they have no known competing financial interests or personal relationships that could have appeared to influence the work reported in this paper.

Ethical approval This article does not contain any studies with human participants or animals performed by any of the authors.

References

Acikel SM, Senay RH, Akgol S, Aslan A (2017) Removal of acid black 210 dye from leather dyeing effluent using spherical particles of P(HEMA-GMA)IDA-Cr(III) hydrogel membrane. J Soc Leather Technol Chem 101:135–142

Ahmed AI, Hay JN, Bushell ME, Wardell JN, Cavalli G (2009) Optimizing halogenation conditions of N-halamine polymers and investigating mode of bactericidal action. J Appl Polym Sci 113:2404–2412

Bai R, Zhang Q, Li L, Li P, Wang YJ, Simalou O, Dong A (2016) N-Halamine-Containing electrospun fibers kill bacteria via a contact/release co-determined antibacterial pathway. ACS Appl Mater Int 8:31530–31540

Cerkez I, Kocer HB, Worley SD, Broughton RM, Huang TS (2012) N-halamine copolymers for biocidal coatings. React Funct Polym 72:673–679

Chen H, Li Q, Wang M, Ji D, Tan W (2020a) XPS and two-dimensional FTIR correlation analysis on the binding characteristics of humic acid onto kaolinite surface. Sci Total Environ 724:138154

Chen W, Zhu Y, Zhang Z, Gao Y, Liu W, Borjihan Q, Dong A (2020b) Engineering a multifunctional N-halamine-based antibacterial hydrogel using a super-convenient strategy for infected skin defect therapy. Chem Eng J 379:122238

Demir B, Broughton RM, Qiao M, Huang TS, Worley SD (2017) N-halamine biocidal materials with superior antimicrobial efficacies for wound dressings. Molecules 22(10):1582

El-Nahhal IM, Zaggout FR, Nassar MA, El-Ashgar NM, Maquet J, Babonneau F, Chehimi MM (2003) Synthesis, characterization and applications of immobilized iminodiacetic acid-modified silica. J Sol-Gel Sci Technol 28(2):255–265

Hanshaw RG, Stahelin RV, Smith BD (2008) Noncovalent keystone interactions controlling biomembrane structure. Chem-Eur J 14(6):1690–1697

Hisaki I, Sasaki T, Tohnai N, Miyata M (2012) Supramolecular-tilt-chirality on twofold helical assemblies. Chem-Eur J 18(33):10066–10073

Huang Y, Zhu Q, Sheng T, Hu S, Fu R, Shen C, Wu X (2013) Lanthanide coordination polymers assembled from triazine-based flexible polycarboxylate ligands and their luminescent properties. CrystEngComm 15(18):3560–3567

Jahangiri A, Ghoreishian SM, Akbari A, Norouzi M, Ghasemi M, Ghoreishian M, Shafiabadi E (2018) Natural dyeing of wool by madder (*Rubia tinctorum* L.) root extract using tannin-based biomordants: colorimetric, fastness and tensile assay. Fiber Polym 19(10):2139–2184

Jiang Z, Ma K, Du J, Li R, Ren X, Huang TS (2014) Synthesis of novel reactive N-halamine precursors and application in antimicrobial cellulose. Appl Surf Sci 288:518–523

Kagarise RE (1955) Spectroscopic studies on the soaps of phenylstearic acid. I. Infrared absorption spectra and the hydrolysis of soap films. J Phys Chem 59(3):196–205

Kang ZZ, Zhang B, Jiao YC, Xu YH, He QZ, Liang J (2013) High-efficacy antimicrobial cellulose grafted by a novel quaternarized N-halamine. Cellulose 20(2):885–893

Kocer HB, Cerkez I, Worley SD, Broughton RM, Huang TS (2011) Polymeric antimicrobial N-halamine epoxides. ACS Appl Mater Inter 3(8):2845–2850

Lai X, Zeng X, Li H, Liao F, Yin C, Zhang H (2012) Synergistic effect between a triazine-based macromolecule and melamine pyrophosphate in flame retardant polypropylene. Polym Compos 33(1):35–43

Li S, Lin X, Liu Y, Li R, Ren X, Huang TS (2019) Phosphorus-nitrogen-silicon-based assembly multilayer coating for the preparation of flame retardant and antimicrobial cotton fabric. Cellulose 26(6):4213–4223

Ma K, Liu Y, Xie Z, Li R, Jiang Z, Ren X, Huang TS (2013) Synthesis of novel N-halamine epoxide based on cyanuric acid and its application for antimicrobial finishing. Ind Eng Chem Res 52(22):7413–7418

Mazik M, Cavga H (2006) Carboxylate-based receptors for the recognition of carbohydrates in organic and aqueous media. J Organ Chem 71(8):2957–2963

Mu T, Pan N, Wang Y, Ren X, Huang TS (2018) Antibacterial coating of cellulose by Iso-bifunctional reactive N-halamine with the dyeing process of reactive dye. Fiber Polym 19(11):2284–2289

Omer AM, Elgarhy GS, El-Subruiti GM, Khalifa RE, Eltaweil AS (2020) Fabrication of novel iminodiacetic acid-functionalized carboxymethyl cellulose microbeads for efficient removal of cationic crystal violet dye from aqueous solutions. Int J Biol Macromol 148:1072–1083

Pan Y, Wang W, Liu L, Ge H, Song L, Hu Y (2017) Influences of metal ions crosslinked alginate based coatings on thermal stability and fire resistance of cotton fabrics. Carbohydr Polym 170:133–139

Razak MR, Yusof NA, Haron MJ, Ibrahim N, Mohammad F, Kamaruzaman S, Al-Lohedan HA (2018) Iminodiacetic acid modified kenaf fiber for waste water treatment. Int J Biol Macromol 112:754–760

Ren X, Kou L, Liang J, Worley SD, Tzou YM, Huang TS (2008) Antimicrobial efficacy and light stability of N-halamine siloxanes bound to cotton. Cellulose 15(4):593–598

Ren X, Kou L, Kocer HB, Worley SD, Broughton RM, Tzou YM, Huang TS (2009) Antimicrobial modification of polyester by admicellar polymerization. J Biomed Mater Res B 89(2):475–480

Richards GN, Zheng G (1991) Influence of metal ions and of salts on products from pyrolysis of wood: applications to thermochemical processing of newsprint and biomass. J Anal Appl Pyrol 21(1–2):133–146

Shi R, Tan L, Zong L, Ji Q, Li X, Zhang K, Xia Y (2017) Influence of Na^{+} and Ca^{2+} on flame retardancy, thermal degradation, and pyrolysis behavior of cellulose fibers. Carbohydr Polym 157:1594–1603

Sosa GL, Zalts A, Ramirez SA (2016) Complexing capacity of electroplating rinsing baths-a twist to the resolution of two ligand families of similar strength. J Anal Sci Technol. https://doi.org/10.1186/s40543-016-0088-3

Sun G, Xu XJ, Bickett JR, Williams JF (2001) Durable and regenerable antibacterial finishing of fabrics with a new hydantoin derivative. Ind Eng Chem Res 40(4):1016–1021

Sun Y, Sun G (2002) Durable and regenerable antimicrobial textile materials prepared by a continuous grafting process. J Appl Polym Sci 84(8):1592–1599

Tian H, Zhai Y, Xu C, Liang J (2017) Durable antibacterial cotton fabrics containing stable acyclic N-halamine groups. Ind Eng Chem Res 56(28):7902–7909

Viola MN, Ikram M, Rehman S, Ali S, Akhtar MN, Aidamen MA, Schulzke C (2019) A paddle wheel dinuclear Copper(II) carboxylate: crystal structure, thermokinetic and magnetic properties. J Mol Struct 1196:754–759

Wang X, Xu M, Zhang Z, Leng Y, Li B (2018) Synthesis of a novel N-alkoxyamine containing compound and its application as an effective flame retardant for polypropylene film by quenching free radical. J Anal Appl Pyrol 134:243–253

Wen W, Zhang Z, Jing L, Zhang T (2020) Synthesis of a Hein-Schiff base compound and its antibacterial activity on cotton fabrics. Cellulose 27(12):7243–7254

Worley SD, Chen Y, Wang JW, Wu R (2005) Novel N-halamine siloxane monomers and polymers for preparing biocidal coatings. Surf Coat Int B 88(2):93–99

Xu D, Ma X, Zhu P, Jiang Z (2020) A novel durable and water-soluble N-halamine precursor for antibacterial cellulose fabrics. AATCC J Res 7(3):34–41

Yin M, Wang Y, Zhang Y, Ren X, Qiu Y, Huang TS (2020) Novel quaternarized N-halamine chitosan and polyvinyl alcohol nanofibrous membranes as hemostatic materials with excellent antibacterial properties. Carbohydr Polym 232:115823

Zhang B, Jiao Y, Kang Z, Ma K, Ren X, Liang J (2013) Durable antimicrobial cotton fabrics containing stable quaternarized N-halamine groups. Cellulose 20(6):3067–3077

Zhang K, Zong L, Tan Y, Ji Q, Yun W, Shi R, Xia Y (2016) Improve the flame retardancy of cellulose fibers by grafting zinc ion. Carbohydr Polym 136:121–127

Zhang Y, Zhu L, Wang Y, Lou Z, Shan W, Xiong Y, Fan Y (2018) Preparation of a biomass adsorbent for gallium(III) based on corn stalk modified by iminodiacetic acid. J Taiwan Inst Chem E 91:291–298

Zhang S, Demir B, Ren X, Worley SD, Broughton RM, Huang TS (2019) Synthesis of antibacterial N-halamine acryl acid copolymers and their application onto cotton. Appl Polym Sci 136(16):47426

Zhou X, Zhou J, Liu Y, Guo J, Ren J, Zhou F (2018) Preparation of iminodiacetic acid-modified magnetic biochar by carbonization, magnetization and functional modification for Cd(II) removal in water. Fuel 233:469–479

Zhu FL, Li X, Feng QQ (2020) Thermal decomposed behavior and kinetic study for untreated and flame retardant treated regenerated cellulose fibers using thermogravimetric analysis. J Therm Anal Calorim. https://doi.org/10.1007/s10973-020-09780-y